A Non-Linear Variational Principle for the Self-Consistent Solution of Poisson's Equation and a Transport Equation in the Local Density Approximation

H. Carrillo-Nuñez
Departement Fysica
Universiteit Antwerpen
Groenenborgerlaan 171
B-2020 Antwerpen, Belgium
Email: hamilton.carillonunoz@ua.ac.be

Wim Magnus
imec, B-3001 Leuven, Belgium
and Departement Fysica
Universiteit Antwerpen
Groenenborgerlaan 171
B-2020 Antwerpen, Belgium

F. M. Peeters
Departement Fysica
Universiteit Antwerpen
Groenenborgerlaan 171
B-2020 Antwerpen, Belgium

***Abstract*—In order to simplify the numerical investigation of carrier transport in nanodevices without jeopardizing the rigor of a full quantum mechanical treatment, we have exploited an existing variational principle to solve self-consistently Poisson's equation and Schrödinger's equation as well as an appropriate transport equation within the scope of the generalized local density approximation (GLDA). In this work, as a benchmark, we have applied our approach to compute the ballistic current density and electron concentration in a Si nanowire.**

I. Introduction

During the last decades, continuous scaling down of device dimensions has resulted in novel generations of electronic devices and structures where the active areas have dimensions in the nanometer range. As quantum effects (e.g. resulting from carrier confinement) may increasingly affect their working principles, ample research is on-going to adequately include the dominant quantum effects into the kinetic equations obeyed by the distribution function. However, the corresponding numerical burden makes this a challenging task, even today when the available computational power is partially countered by the increased complexity of nano-scale devices.

As a test case for this study, we consider an ultra-thin cylindrical MOSFET depicted in Fig. 1. The structure consists of a semiconductor nanowire which is covered by an oxide layer whereas a gate contact overlays the p-doped channel region, the latter being sandwiched between heavily n-doped source and drain regions. This device has been the subject of various theoretical[1], [2] studies and is considered a promising candidate to replace the convectional planar MOSFET[3].

In this work, we address a quantum mechanical transport model consisting of a simplified Poisson-Schrödinger solver and a module to compute the current density, all within the framework of the generalized local density approximation (GLDA)[4]. Furthermore, the 1D ballistic Boltzmann transport equation (BTE) has been solved within the framework of the GLDA in order to calculate self-consistently the carrier distribution and the potential profile felt by the carriers as well as the current flowing through the conduction channel inside the nanowire. Unlike previous formalisms[1], [5], [6], [7], we have invoked a variational scheme[8] in order to avoid the necessity of going back and forth between the Schrödinger and Poisson equations.

Section II is devoted to the non-linear variational principle which is the cornerstone of the simplified Poisson-Schrödinger solver, whereas the latter is discussed in section III together with its numerical implementation. In section IV an expression for the ballistic current density is given which is based on an analytical solution of the collision-free BTE. A few results are shown and discussed in V and a summary of this work is presented in section VI.

II. Non-linear variational principle

As is well known, the solution of Poisson's equation

$$\epsilon\nabla^2 V(\mathbf{r}) = -\rho(\mathbf{r}) \tag{1}$$

for a fixed charge density profile $\rho(\mathbf{r})$ amounts to minimizing a proper action functional S with respect to V, i.e.

$$\delta S = 0, \quad S \equiv \int \mathrm{d}^3 r \left[\epsilon|\nabla V(\mathbf{r})|^2 - \rho(\mathbf{r})V(\mathbf{r})\right]. \tag{2}$$

In a real device however, the density is itself a complicated functional of the potential through the distribution function and the wave functions that are directly affected by the potential. Therefore, also the corresponding constitutive transport equations need to be solved self-consistently with Poisson's equation. Equivalently, the self-consistent solution can be seen to emerge from the non-linear Poisson equation

$$\epsilon\nabla^2 V(\mathbf{r}) = -\rho[\mathbf{r}, V]. \tag{3}$$

In the particular case where $\rho[\mathbf{r}, V]$ depends only on the local potential in the point r, i.e. $\rho[\mathbf{r}, V] = \rho[\mathbf{r}, V(\mathbf{r})]$, we may

978-1-4244-7700-5/10/$26.00 ©2010 IEEE

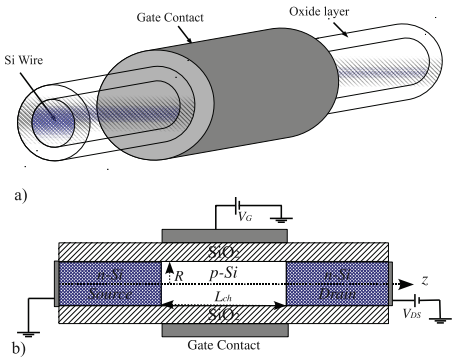

Fig. 1. Schematic picture of the cylindrical MOSFET: a) 3D view and b) cross-sectional view of the device.

generalize Eq. (2) according to

$$S = \int \mathrm{d}^3 r \left[\epsilon |\nabla V(\mathbf{r})|^2 - \int_{V_0}^{V(\mathbf{r})} \mathrm{d}V' \rho[\mathbf{r}, V'] \right], \qquad (4)$$

where, the total charge density contains the usual contributions from electrons, holes and ionized impurities.

$$\begin{aligned} \rho\big[r, V(\mathbf{r})\big] \;=\; & e\Big(p\big[r, V(\mathbf{r})\big] - n\big[r, V(\mathbf{r})\big] \\ & + N_{\mathrm{D}}^{+}\big[r, V(\mathbf{r})\big] - N_{\mathrm{A}}^{-}\big[r, V(\mathbf{r})\big] \Big). \end{aligned} \qquad (5)$$

The solution to Eq. (3) is obtained directly when $\delta S = 0$. Moreover, it can be shown that the extreme value corresponding to $\delta S = 0$ is an absolute minimum provided $\partial\rho/\partial V > 0$ for all possibles values of the dummy potential V. The requirement that the density is a local functional of V is fulfilled in case the GLDA [4] is adopted and the energy eigenvalues as well as the distribution function depend locally on relatively smooth potential variations while confinement effects are rigorously accounted for. Whereas the above mentioned non-linear variational principle is applied in Ref. [8] to derive analytical expressions for the quasi-Fermi potential in erasable memory devices, we have exploited it: 1) as an iterative algorithm to solve the non-linear Poisson equation, thereby avoiding the necessity of going back and forth between Poisson's equation and the kinetic equations/Schrödinger equation, and 2) as an absolute convergence criterion. As to the latter, it should be noted that the numerically calculated action always exceeds the absolute action minimum corresponding to the exact solution. Consequently, tracing back the action flow during the iteration loop, we may estimate the stability of the solution emerging from relative convergence between two subequent iterations, as a stable solution should correspond to a action that is still decreasing.

III. Self-consistent Poisson-Schrödinger solver

A. Electron Concentration within the GLDA

In case of a cylindrical wire the potential energy profile $U(r,z)$ consists of the electrostatic potential energy $U_e(r,z) = -eV(r,z)$ obtained by solving self-consistently the Schrödinger and Poisson equations, and the abrupt energy barrier $U_B(r,z) = U_{\mathrm{B}}\,\Theta(r > R)$ at the semiconductor/oxide interface $r = R$. Taking the barrier height U_{B} infinitely high for the sake of simplicity, we assume that all electrons are confined to the interior of the nanowire. Consequently, for an homogeneous and unbiased perfect cylindrical wire without junctions, within the framework of the effective-mass approximation, the electron eigenfunctions $\psi_{\alpha ml}(k; r, \phi, z)$ and the corresponding energy eigenvalues $E_{\alpha ml}(k)$ can be expressed analytically as follows:

$$\begin{aligned} E_{\alpha ml}(k) &= \frac{\hbar^2 k^2}{2m_{\alpha z}} + \frac{\hbar^2 x_{ml}^2}{2m_{\alpha\perp} R^2}, \quad m = 0, \pm 1, \pm 2, \ldots; \\ & \qquad\qquad\qquad\qquad l = 1, 2, \ldots \\ \psi_{\alpha ml}(k; r, \phi, z) &= \frac{J_m\left(\frac{x_{ml} r}{R}\right) \mathrm{e}^{\mathrm{i}m\phi} \mathrm{e}^{\mathrm{i}kz}}{\sqrt{\pi R^2 L}\,|J_{m+1}(x_{ml})|}, \end{aligned} \qquad (6)$$

where L is the wire length and x_{ml} the $l-$th zero of the m-th Bessel function $J_m(x)$. In the latter, α is a conduction band valley index whereas $m_{\alpha\perp}$ and $m_{\alpha z}$ respectively denote the effective mass in the planar cross section of the wire and the longitudinal effective mass in the transport direction.

On the other hand, a non-uniform potential energy profile $U_e(r,z)$ emerges inside a gated nanowire consisting of an n^+–p^-–n^+ structure and being biased by both a gate voltage V_{G} and a drain voltage V_{ds}. Adopting both the Hartree approximation and the GLDA[4], the second assuming that the variation of $U_e(r,z)$ in both the r- and z-directions is sufficiently small on the scale of the Fermi wave-length, we may write the electron concentration inside the biased wire as

$$\begin{aligned} n(r,z) = \; & \sum_{m=0}^{\infty} \sum_{l=1}^{\infty} C_{ml} J_m^2 \left(\frac{x_{ml} r}{R}\right) \\ & \times \sum_{\alpha} \int_{-\infty}^{\infty} \mathrm{d}k\, f_{\mathrm{B}}(E_{\alpha ml}(k) - eV(r,z)). \end{aligned} \qquad (7)$$

Here, we have simply added $U_e(r,z)$ to the unperturbed one-electron eigenenergies $E_{\alpha ml}(k)$ thereby keeping the wave functions $\psi_{\alpha ml}(k; r, \phi, z)$ unaltered, whereas $f_{\mathrm{B}}(E)$ is taken to be the ballistic electron distribution function for the steady state:

$$f_{\mathrm{B}}(E) = F(E, \mu(r, z, \hbar k)). \qquad (8)$$

The chemical potential $\mu(k, r, z)$ conveniently expressed in terms of the logical step function $\Theta(x)$:

$$\begin{aligned} \mu(r,z,p) = E_{\mathrm{F}} - eV_{\mathrm{ds}} \Big[& \Theta\big(p \le -p_{\mathrm{M}}(r,z)\big)\Theta\big(z \le z_{\mathrm{M}}(r)\big) \\ & + \Theta\big(p \le p_{\mathrm{M}}(r,z)\big)\Theta\big(z \ge z_{\mathrm{M}}(r)\big) \Big] \end{aligned} \qquad (9)$$

In Eq.(8), $F(E, E_{\mathrm{F}}) = [1 + \exp\big(\beta(E - E_{\mathrm{F}})\big)]^{-1}$ is the Fermi-Dirac distribution function, E_{F} the Fermi energy, and $\beta = 1/k_{\mathrm{B}}T$. The normalization coefficients C_{ml} are given by $C_{ml} = (2 - \delta_{m0})/(\pi^2 R^2 J_{m+1}^2(x_{ml}))$.

Having solved the Schrödinger equation in the GLDA approximation for the radial and azimuthal subbands, we have invoked the Lagrange–Charpit method using classical

trajectories [9], [10], [11] as the characteristic curves of the Boltzmann equation to construct the ballistic distribution function, Eqs. (8)-(9), as a local functional of $U_e(r,z)$. The solution relies on the assumption that, for a given coordinate $r \leq R$, the potential energy attains a unique maximum in the z-direction $U_{\rm M}(r)$ at some point $z_{\rm M}(r)$, allowing to define a "critical momentum" $p_{\rm M}(r,z) = \sqrt{2m_{\alpha z}\big(U_{\rm M}(r) - U_e(r,z)\big)}$.

B. Electron density action

The action S in Eq. (3) essentially contains five terms, $S = S_0 + S_1 + S_2 + S_3 + S_4$. S_0 is the contribution of the first term in the second part of Eq. (3). The other four terms are related to the contributions from the electron, hole, donor and acceptor densities, respectively. Carrying out the integration over V', we can easily find the contribution of the electron density to the action, which is given by

$$S_1 = \frac{1}{\beta}\sum_{m=0}^{\infty}\sum_{l=1}^{\infty} C_{ml}\int_0^R {\rm d}r\, r J_m^2\Big(\frac{x_{ml}r}{R}\Big)\int_0^L {\rm d}z \times \sum_{\alpha}\int_{-\infty}^{\infty}{\rm d}k \ln\Big[1+{\rm e}^{\beta\left(\mu(r,z,\hbar k)-E_{\alpha ml}(k)+eV(r,z)\right)}\Big], \tag{10}$$

where the contribution related to the constant V_0 has been omitted. The other three contributions can be calculated in a similar way.

In order to evaluate the action, we define a 2D-grid of (r_i, z_j) points with $0 \leq i \leq N_r$ and $0 \leq j \leq N_z$. Providing an educated initial guess for the potential $V(r_i, z_j)$, we extract the charge density from the set of equations (5) to (7). Substituting the charge density into the discretized Poisson equation we calculate a new potential using a Gauss-Seidel iteration scheme[12] until the criterion of convergence, $\delta S = 0$, is reached.

IV. Current density within GLDA

The ballistic electron current density can be obtained as the group velocities $p/m_{\alpha z}$ average with the distribution function given by Eqs.(8)-(9). Consequently, it is found that only electrons surmounting the barrier maximum $U_{\rm M}(r)$, or equivalently carrying out momenta $|p| > p_{\rm M}(r,z)$ can contribute to the current. Moreover, it can be shown that $J(r)$ is independent of z and analytically expressed as:

$$J(r) = \frac{e}{2\pi\hbar\beta}\sum_{m=0}^{\infty}\sum_{l=1}^{\infty} C_{ml} J_m^2\Big(\frac{x_{ml}r}{R}\Big) \times \sum_{\alpha}\ln\left[\frac{1+{\rm e}^{\beta(E_{\rm F}-U_{\rm M}(r)-W_{\alpha ml})}}{1+{\rm e}^{\beta(E_{\rm F}-U_{\rm M}(r)-W_{\alpha ml}-eV_{\rm ds})}}\right], \tag{11}$$

in accordance with the requirement that the steady-state current density be solenoidal. The total current passing through the cross-section of the nanowire can be computed by integrating $J(r)$ over the wire cross section. It follows from Eq. (11) that, at low temperatures ($\beta \to \infty$), when only the lowest subband is occupied by electrons, and for low drain voltages ($eV_{\rm ds} \ll E_F$) the current obtained by integrating Eq.(11) reduces to the Landauer-Büttiker formula[7] with full transmission.

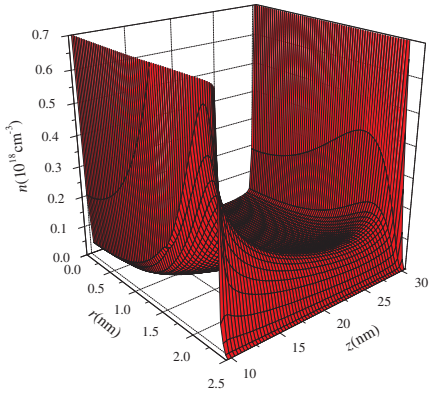

Fig. 2. 3D electron concentration at $V_{\rm ds}$ = 0.3 V, with $L_{\rm CH} = 20$ nm.

V. Results

For the numerical simulation of a cylindrical MOSFET, we have taken the longitudinal and transverse electron masses to be $m_{\rm trans} = 0.19\, m_0$ and $m_{\rm long} = 0.98\, m_0$ respectively, and we have chosen the following values for the device parameters: the nanowire radius and the thickness of the SiO_2 layer are taken to be R = 2.5nm and 1.5nm, respectively; the dielectric constant of silicon and the oxide layer are respectively given by $\epsilon_{\rm Si} = 11.7$ and $\epsilon_{\rm ox} = 3.9$; the channel length $L_{\rm CH}$ equals 20 nm, while the length of the uniformly doped source and drain contacts is fixed to 10 nm. The donor concentration of both regions is $N_{\rm D} = 10^{20}$ cm^{-3} whereas the p-doped channel has an acceptor concentration $N_{\rm A} = 10^{18}$ cm^{-3}. The temperature is 300 K and the current-voltage characteristics shown below are calculated for the gate voltages $V_{\rm G}$ ranging from 0 to 0.7 V, the drain voltage $V_{\rm ds} = 0.1$ V and 0.3 V. The action functional that was minimized numerically with respect to $V(r,z)$ (see Eqs. (3)-(10)), has been computed as the sum of all contributions arising from $N_r \times N_z$ rectangular grid cells, with N_r = N_z = 120. In each cell the Laplace operator in r and z has been discretized according to the method of finite differences. The simulation normally takes less than 5 min per bias point on one regular desktop.

Fig. 2 depicts a typical electron concentration in the channel region for a drain voltage $V_{\rm ds} = 0.3$ V and gate voltage $V_{\rm G}$ =0.7 V, where the inversion layer electrons in the radial direction, is located near the Si/SiO_2 interface at $r = R$. The electron concentration is found to pile up pronouncedly in front of the latter interface while vanishing completely at $r = R$. This result can be observed similarly in Fig. 3 where is plotted the 3D current density computed for $V_{\rm G} = 0.7$ V, as function of r and $V_{\rm ds}$. Note that the current density at the center of the nanowire takes considerably lower values than in the inversion layer where most of the electrons are located while, due to the confinement, the current density is bound to vanish at the Si/SiO_2 interface.

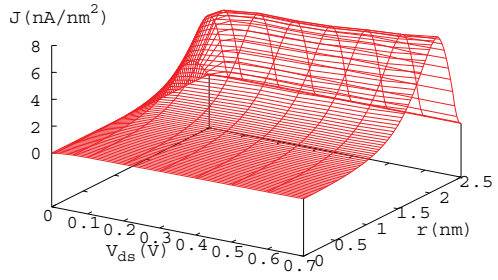

Fig. 3. 3D current density at $V_{\rm G}$ =0.7 V.

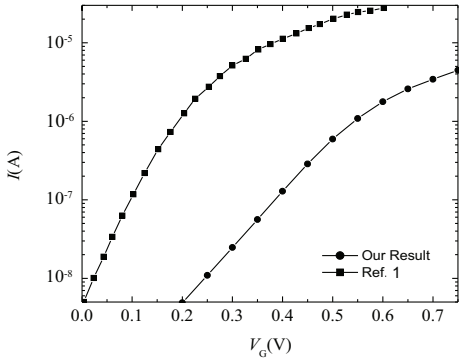

Fig. 4. The I-$V_{\rm G}$ characteristics for an intrinsic Si nanowire. The device parameters and doping concentration are obtained from Ref. [1] as: R=1.5nm, $L_{\rm CH}$=10nm, 8nm for the source and drain lenght and $N_{\rm D}$=$2 \times 10^{20} cm^{-3}$.

In order to compare with previous results, in Fig. 4 we have plotted the I-$V_{\rm G}$ characteristics obtained by implementing our approach and similar characteristics reported by Wang *et-al* in Ref. [1]. As can be observed, both curves are in qualitative agreement, while the main quantitative differences can be explained by noticing that our approach presently ignores both reflection and tunneling events as well as the metal gate /semiconductor work function difference, amounting to approximately 0.25 eV. Systematic comparison between the present approach and existing Poisson – Schrödinger solvers need to be made in the future to estimate the gain in CPU time. Meanwhile, as the Schrödinger equation is solved only once, we believe that the average simulation time will not exceed that of a purely classical treatment based on Boltzmann statistics.

VI. CONCLUSION

Based on a non-linear variational principle, a numerical algorithm was developed to directly integrate the Poisson equation and the Schrödinger equation as well as the constitutive transport equations within the framework of the GLDA. The algorithm not only offers a trade-off between quantum mechanical rigor and computational speed, but also accelerates the evaluation of quantum mechanical charge and current density profiles of devices for which the GLDA is an acceptable approximation.

ACKNOWLEDGMENT

This work was supported by Flemish Science Fundation (FWO-VI) and the Interuniversity Attraction Poles, Belgium State, Belgium Science Policy, and imec.

REFERENCES

[1] J. Wang, E. Polizzi, and M. Lundstrom, "A three-dimensional quantum simulation of silicon nanowire transistors with the effective mass approximation," *J. Appl. Phys.*, vol. 96, no. 4, pp. 2192–2203, May 2004.

[2] S.N. Balaban, E. Pokatilov, V. Fomin, V. Gladilin, J. Devreese, W. Magnus, W. Schoenmaker, M. V. Rossum, and B. Sorée, "Quantum trasnport in a cylindrical sub-0.1 μm silicon-based mosfet," *Solid-state Electron.*, vol. 46, no. 3, pp. 435–444, Feb. 2002.

[3] L.J. Lauhon, M. Gudiksen, D. Wang, and C. Lieber, "Epitaxial core–shell and core–multishell nanowire heterostructures," *Nature (London)*, vol. 420, no. 6911, pp. 57–61, Nov. 2002.

[4] G. Paasch and H. Übensee, "A modified local density approximation. electron density in inversion layers," *Phys. Status Solidi B*, vol. 113, no. 1, pp. 165–178, May 1982.

[5] M.D. Croitoro, V. Gladilin, V. Fomin, J. Devreese, W. Magnus, W. Schoenmaker, and B. Sorée, "Quantum transport in a nanosize double-gate metal-oxide-semiconductor field-effect transistor," *J. Appl. Phys.*, vol. 96, no. 4, pp. 2305–2310, Aug. 2004.

[6] S. Barraud, "Phase-coherent quantum transport in silicon nanowires based on wigner transport equation: Comparison with the nonequilibrium-green-function formalism," *J. Appl. Phys.*, vol. 106, no. 6, p. 063714, Sept. 2009.

[7] S. Datta, *Electronic transport in Mesoscopic Systems*. Cambrigde University Press, Cambridge, UK, 1997.

[8] C.-Y. Lee and C.-K. Kim, "Variational formulation of poisson's equation in semiconductor at quasi-equilibrium and its applications," *IEEE Trans. Electron Devices*, vol. 44, no. 9, pp. 1507–1513, Sept. 1997.

[9] F. Brosens and W. Magnus, "Carrier transport in nanodevices: revisiting the boltzmann and wigner distribution functions," *Phys. Status Solidi B*, vol. 246, no. 7, pp. 1656–1661, July 2009.

[10] M.J Cáceres, J. Carrillo, I. Gamba, A. Majorana, and C.-W. Shu, "Dsmc versus weno-bte: A double gate mosfet example," *J. Comput. Electron.*, vol. 5, no. 4, pp. 471–474, Dec. 2006.

[11] M.J Cáceres, J. Carrillo, and T. Goudon, "Equilibration rate for the linear inhomogeneous relaxation-time boltzmann equation for charged particles," *Commun. PDE*, vol. 28, no. 5 & 6, pp. 969–989, Jan. 2003.

[12] W. Press, B. Flannery, S. Teukolsky, and W. Vetterling, *Numerical Recipes in Fortran 77: The art of Scientific Computing*. Cambrigde University Press, Cambridge, UK, 1992.